# Isotope Exchange Measurements of the Interfacial Reaction Rate Constant of Nitrogen on Fe-Mn alloys and an Advanced High-Strength Steel

DAI TANG and PETRUS CHRISTIAAN PISTORIUS

Precise control of dissolved nitrogen is required for producing Third-Generation Advanced High-Strength Steels (AHSS). Compared with well-documented thermodynamic data, the data on the kinetics of nitrogen dissolution in these steels are limited. The isotope exchange technique ($^{15}N$–$^{14}N$ exchange reaction) was applied to measure the nitrogen reaction rate at different temperatures, on pure liquid iron, liquid iron containing different levels of manganese, and liquid Fe-Mn-Al-Si steel with a Third-Generation AHSS composition. The increase in the interfacial reaction rate with increased temperature corresponded to an activation energy of 144.2 kJ/mol for pure iron. For Fe-Mn alloy, the interfacial reaction rate increased with the increased temperature and increased manganese content. For liquid AHSS (Fe-Mn-Al-Si), the interfacial reaction rate was approximately one third of the rate for pure liquid iron, at the same temperature, with a corresponding activation energy of 160.5 kJ/mol.

https://doi.org/10.1007/s11663-020-01999-2


## I. INTRODUCTION

NITROGEN in steel exists as free dissolved nitrogen and compounds (nitrides and carbonitrides).[1] Uncombined nitrogen in solid steel forms an interstitial solute. Nitrogen may enhance the strength of steel products by precipitation strengthening, but it is also well known for its aging and embrittling effect. Precise control of nitrogen during the steelmaking process would contribute to improved mechanical behavior of advanced high-strength steel (AHSS) grades.

Compared to the comprehensive thermodynamic data (such as nitrogen solubility in liquid steel with different levels of alloy elements and interaction parameters between nitrogen and alloy elements), kinetic data about nitrogen reactions are still limited. The interfacial reaction rate between nitrogen and the liquid Third-Generation AHSS is of particular interest, as these steels have high concentrations of alloying elements such as Mn (up to 10 pct), Al, and Si (both up to 3 pct).[1]

The affinities of these alloy elements for nitrogen differ from that of liquid iron. It was previously reported that the affinities of alloy elements for nitrogen (thermodynamic effect) correlate with the effect of the alloying elements on the interfacial nitrogen reaction rate (kinetic effect).[2–4]

The process of nitrogen transfer in the atmosphere to or from liquid steel includes gas phase transfer, interfacial reactions, and nitrogen transfer in the liquid steel. Nitrogen transfer in liquid steel can be limiting, especially for steels with rapid interfacial reactions, such as those with low sulfur concentrations, or containing alloying elements such as chromium.[5] In such cases (limited by liquid mass transfer), the interfacial reaction rate cannot be accurately determined from the nitrogen pick-up rate.

To avoid the influence of limited liquid phase mass transfer, the isotope exchange technique proposed by Byrne and Belton[6] was applied to measure the interfacial reaction rate between nitrogen and liquid steel containing different alloying elements.

Nitrogen has two stable isotopes: $^{14}N$ and $^{15}N$. $^{14}N$ is dominant, making up 99.634 pct of natural nitrogen. As a result, most $N_2$ molecules have a molecular mass of 28, which is represented as $^{28}N_2$. $^{30}N_2$, with a molecule mass of 30, is stable and can be enriched and preserved separately.

The nitrogen isotope exchange experiment is based on atomic exchange between nitrogen molecules at the liquid steel surface. A certain portion of $^{30}N_2$ is added to a main flow of $^{28}N_2$. The flow of $^{30}N_2$-enriched nitrogen

DAI TANG is with Nucor Steel Decatur, 4301 Iverson Blvd, Trinity, AL 35673, USA and also with the Department of Materials Science and Engineering, Carnegie Mellon University, Pittsburgh, PA 15213. PETRUS CHRISTIAAN PISTORIUS is with the Department of Materials Science and Engineering, Carnegie Mellon University. Contact e-mail: pistorius@cmu.edu.

Manuscript submitted June 26, 2020 and accepted October 2, 2020.
Article published online October 27, 2020.

is directed at the liquid steel surface, which provides active metal sites for atomic exchange between nitrogen molecules.[5, 6]

When the liquid steel is saturated with nitrogen, the dissociation and association of nitrogen molecules at the liquid steel surface reach a dynamic equilibrium. The dissociation of nitrogen molecules into two nitrogen atoms is considered the rate-limiting step of the nitrogen-liquid steel interfacial reaction. $^{28}N_2$ and $^{30}N_2$ molecules split into individual nitrogen atoms ($^{14}N$ and $^{15}N$) that recombine randomly to form $^{28}N_2$, $^{29}N_2$, and $^{30}N_2$ molecules. The process is termed 'nitrogen isotope exchange'. The concentrations of $^{30}N_2$ in the incoming and product gas streams can be analyzed with a residual gas analyzer (RGA). A residual gas analyzer is a mass spectrometer that measures the composition of a gas flow present in a low-pressure environment. The RGA ionizes individual components of the gas mixture and then detects and determines the mass-to-charge ratios ($m/z$). The species $^{30}N_2^+$ can be separated readily from $^{28}N_2^+$ and $^{29}N_2^+$ with a well-tuned RGA with a reasonable resolution.

## II. EXPERIMENTAL METHOD

A high-frequency induction furnace, with a fused-quartz working tube (OD 85 mm, ID 80 mm, length 400 mm) and end caps to control the furnace atmosphere, was used for these experiments. A graphite crucible (OD 70 mm, ID 64 mm) was placed in the hot zone for induction heating. A closed-end $Al_2O_3$ tube (OD 19.05 mm, ID 12.7 mm, length 305 mm) was used as both the reactor of the isotope exchange process and the gas outlet. Approximately 20 g of electrolytic iron (Alfa Aesar Purity: 99.99 pct, containing < 0.0030 pct S based on Alfa Aesar Certificate), or electrolytic iron mixed with alloying elements (Al: shot, Alfa Aesar, Purity: 99.99 pct, Si: pieces, Alfa Aesar, Purity: 99.95 pct and Mn: irregular pieces, Alfa Aesar, 99.9 pct) was put into the tube before the experiment. A B-type thermocouple was positioned adjacent to the bottom of the closed-end $Al_2O_3$ tube containing the steel sample to monitor the temperature. Another open-ended $Al_2O_3$ tube with a smaller diameter (OD 6.35 mm, ID 4.78 mm) was used as the gas inlet and inserted into the closed-end $Al_2O_3$ tube. The distance between the end of the inner tube and the liquid metal surface was set at 5 mm. The bottom part of the outer tube (reactor) was placed inside the graphite crucible (susceptor) for induction heating. Figure 1 is a schematic of the induction furnace setup for these nitrogen isotope exchange experiments.

Argon (at approximately 300 mL/min [for reference conditions of 294 K and 1 atm pressure, as are all the flow rates reported here]) flowed through the fused-quartz tube to protect the graphite crucible from oxidation. The nitrogen-hydrogen mixture flowed through the smaller alumina tube onto the surface of the liquid metal; different flow rates were tested first (discussed in the following section). A flow rate of 50

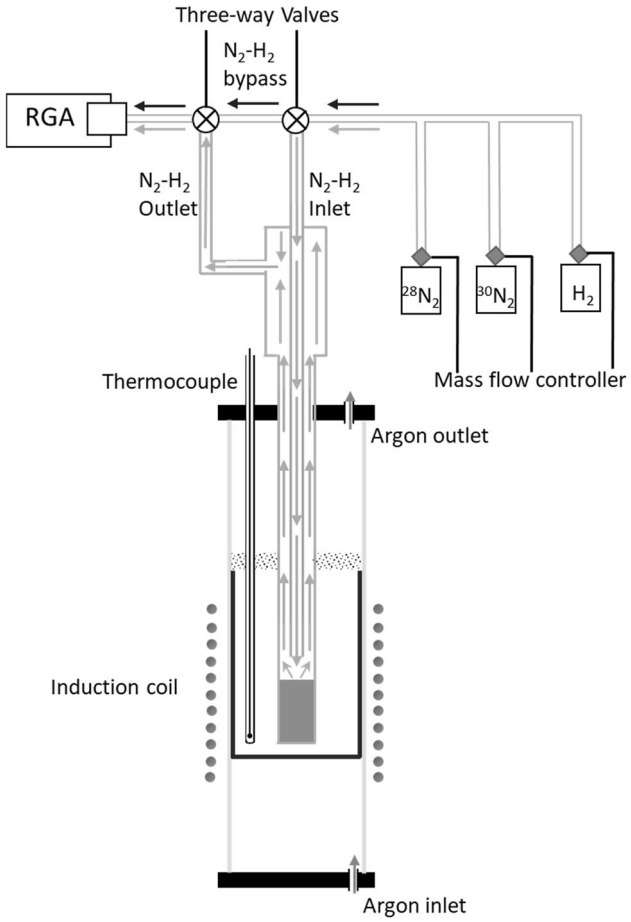


Fig. 1—Schematic of the induction furnace setup for the nitrogen isotope exchange experiment.

mL/min of natural abundance $N_2$ (research purity 99.9999 pct) and 10 mL/min $H_2$ (research purity 99.9999 pct) was selected.

Oxygen or water vapor in the gas stream can be detrimental to these experiments since dissolved oxygen blocks the nitrogen reaction on the liquid steel surface. Belton and Byrne measured an impact factor of 220 for dissolved oxygen in iron, which means 45 ppm oxygen can halve the nitrogen reaction rate.[6]

For this reason, $H_2$ was included to remove oxygen from the liquid steel surface. Heated magnesium turnings were used as oxygen getter; copper turnings should be avoided since hydrogen would reduce oxidized copper turnings and form water vapor. After the metal was heated up to the target temperature, $^{30}N_2$ (Sigma-Aldrich, purity 98 pct) was added into the gas flow (directed at the metal surface) at approximately 1 mL/min. The flow rate of natural abundance $N_2$ remained 50 mL/min and that of $H_2$ remained 10 mL/min. The partial pressure of gases was monitored during the whole experiment with a Residual Gas Analyzer (LC-D Series Residual Gas Analyzer, AMETEK Process Instruments) connected to the gas outlet. There is a response time for $^{30}N_2$ to be detected by the Residual Gas Analyzer (RGA). After 20 min, found to be long enough to attain a stable partial pressure of $^{30}N_2$, the

incoming fraction of $^{30}N_2$ was measured by passing the flow directly to the gas analyzer by means of a bypass circuit. By switching back and forth between the bypass circuit and the furnace circuit, the fraction of $^{30}N_2$ in the gas mixture before and after the reaction ($^{30}F_i$ and $^{30}F_f$) was measured. For each condition (bypass or over liquid metal), $^{30}F_i$ and $^{30}F_f$ were calculated using an average of the data that had been recorded for one minute.

Five experiments are documented here (Table I): Exp. I was a blank experiment, testing whether measurable isotope exchange would happen inside the reactor (an empty $Al_2O_3$ tube); Exp. II tested the effect of the total flow rate on the measured interfacial reaction rate; Exp. III tested the temperature dependence of the measured interfacial reaction rate for pure liquid iron; Exp. IV tested the effect of [Mn] in the liquid steel on the interfacial reaction rate; Exp. V measured the interfacial reaction rate for liquid steel with a Third-Generation AHSS composition. The Al level selected in Exp. V (0.5 wt pct) stayed at the lower end of the Third-Generation AHSS composition range (0 to 4 wt pct).[1] This is because AlN will form in the liquid at 1600 °C if the Al content is higher than 0.5 wt pct, for equilibrium with the nitrogen-rich gas used in these experiments.

Compared with Byrne and Belton's classic experiments, the three major modifications of the current experimental setup were as follows: (i) a bypass gas line was added to directly measure the baseline $^{30}N_2$ concentration. During experiments, a mismatch between the $^{30}N_2$ concentration calculated based on the readings from mass flow controllers and readings from RGA were observed occasionally. By adding a bypass line, the $^{30}N_2$ concentration before and after the reaction could be measured directly. (ii) A graphite susceptor was placed between the induction coil and the tube containing the steel melt. The graphite susceptor was inductively heated, transferring heat to the steel melt by radiation, giving a stable experimental temperature. (iii) The reactor containing the sample was a closed-end ceramic tube, facilitating atmosphere control.

### A. *Calculations*

The overall isotope exchange reaction at the liquid metal surface can be expressed as follows:

$$^{28}N_2 + {}^{30}N_2 = 2{}^{29}N_2 \quad [1]$$

Byrne and Belton derived the following equations to calculate the apparent rate constant ($k^a$) for Eq. [1][6]:

$$k^a = -\frac{\bar{V}}{AR_sT}\ln\frac{{}^{30}F_f - {}^{15}f{}^{15}f}{{}^{30}F_i - {}^{15}f{}^{15}f} \quad [2]$$

where $\bar{V}$ is the volumetric flowrate of the inlet gas mixture (containing $^{30}N_2$, $^{28}N_2$ and $H_2$) at the temperature $T$ (the flow rate of $^{30}N_2$ was calculated based on the measured ratio of $m/z$ 30 to $m/z$ (28 + 29) in the off-gas, as $m/z$ (28 + 29) represents the partial pressure of $^{28}N_2$ + $^{28}N_2H^+$, as discussed later; the flow rate of $H_2$ was 10 mL/min and that of $^{28}N_2$ was 50 mL/min). $A$ is the reaction surface area (equal to the cross-sectional area of the reactor), and $R_s$ is the ideal gas constant (equal to 82.1 $cm^3$ atm $K^{-1}$ $mol^{-1}$ for $k^a$ in mol $cm^{-2}$ $s^{-1}$ $atm^{-1}$). $^{30}F_i$ and $^{30}F_f$ are the fractions of $^{30}N_2$ in the gas mixture before and after the isotope exchange reaction and can be calculated based on the abundance (partial pressure) of species with different mass-to-charge ratios ($m/z$) in the mass spectrum:

$${}^{30}F = \frac{P_{30N_2}}{P_{28N_2} + P_{29N_2} + P_{30N_2}} = \frac{{}^{30}I}{{}^{28}I + {}^{29}I + {}^{30}I} \quad [3]$$

where $^{28}I$, $^{29}I$, and $^{30}I$ are intensities of peaks at ($m/z$) of 28, 29, and 30, read directly from RGA.

$^{14}f$ and $^{15}f$ are $^{14}N$ and $^{15}N$ atomic fractions in the system of nitrogen molecules:

$${}^{14}f + {}^{15}f = 1 \quad [4]$$

$^{15}f$ $^{15}f$ represent the equilibrium fraction of $^{30}N_2$ in the system of nitrogen molecules[6]:

$${}^{30}F_{eq} = {}^{15}f{}^{15}f \quad [5]$$

In principle, $k^a$ can also be calculated from the change in the concentration of $^{29}N_2$, as follows:

$$k^a = -\frac{\bar{V}}{AR_sT}\ln\frac{{}^{29}F_f - 2{}^{14}f{}^{15}f}{{}^{29}F_i - 2{}^{14}f{}^{15}f} \quad [6]$$

Similarly, $2{}^{14}f$ $^{15}f$ represents the equilibrium fractions of $^{29}N_2$ in the system of nitrogen molecules:

$${}^{29}F_{eq} = 2{}^{14}f{}^{15}f \quad [7]$$

Comparing Eqs. [6] to [2], for the same apparent rate constant $k^a$, the change of the fraction of $^{29}N_2$ should be larger than that of $^{30}N_2$. This is because $2{}^{14}f{}^{15}f$ is much larger than $^{15}f{}^{15}f$ (generally $^{15}f$ is less than 3 pct in the gas mixture, and $^{14}f$ is more than 97 pct) and $^{29}F_i$ is close to zero.

However, direct measurement of the $^{29}N_2$ was not possible because protonated molecular $N_2H^+$ forms within the ion source of the RGA by interaction of the electron beam with $H_2$ molecules. Protonated molecular $N_2H^+$ forms through the following two reactions:

**Table I. Experimental Conditions for Isotope Exchange Experiments**

| | Temperature (°C) | Flow rate of $N_2$–$H_2$ mixture (mL/min) | Compositions (wt pct) |
|---|---|---|---|
| Exp. I Empty $Al_2O_3$ Tube | 1650 | 60 | |
| Exp. II Effect of the Total Flow Rate | 1650 | 60 75 90 | pure liquid iron |
| Exp. III Effect of Temperature | 1600 1650 1700 | 60 | pure liquid iron |
| Exp. IV Effect of Manganese | 1600 1650 1700 | 60 | 0 6 10 Mn |
| Exp. V $k^c$ for the 3rd Gen AHSS | 1600 1650 1700 | 60 | 0.5 Al 1.5 Si 6 Mn 92 Fe |

$$N_2 + H^+ \leftrightarrow N_2H^+ \quad [8]$$

$$N_2 + H_3^+ \leftrightarrow N_2H^+ + H_2 \quad [9]$$

At room temperature, the standard Gibbs free energy change for Reaction [8] is negative (− 464.5 kJ/mol[7]) and the reaction can occur spontaneously. Reaction [9] is also spontaneous as $N_2$ has a higher proton affinity than $H_2$.[7] Both of the reactions lead to the formation of $N_2H^+$, which has an ($m/z$) of 29 (the same as $^{29}N_2^+$). Because of $N_2H^+$ formation, the measured intensity for ($m/z$) 29 is a combination of $^{29}N_2H^+$ and $^{29}N_2^+$.

Figure 2 shows that ($m/z$) 29 intensity relative to ($m/z$) 28 intensity is proportional to the fraction of $H_2$ in the mixed gas (balance $N_2$). This is because the intensity of the $m/z$ = 29 peak is dominated by $^{29}N_2H^+$ which is itself determined by the concentrations of $H^+$ and $H_3^+$ inside the ion source (when there is abundant $^{28}N_2$). For this reason, the formation of $^{29}N_2$ is undetectable with the gas composition used in these experiments; instead, the change in $^{30}N_2$ (intensity of $m/z$ = 30 peak) was used to determine the interfacial reaction rate.

The measured (apparent) rate constants were corrected for the effect of limited gas phase mass transfer:

$$\frac{1}{k^c} = \frac{1}{k^a} - \frac{RT}{k^g} \quad [10]$$

Here, $k^c$ is the nitrogen-liquid Fe (or Fe-Mn/Fe-Mn-Si-Al) interfacial reaction rate constant (in mol cm$^{-2}$ s$^{-1}$ atm$^{-1}$), $k^g$ is the gas phase mass transfer coefficient (which depends on the experimental geometry and gas flow rate), calculated using the correlations of Saito *et al.* [8]:

$$k^g(\text{in m s}^{-1}) = \text{Sh}\frac{D_{N_2-H_2}}{d_c} \quad [11]$$

where Sh is Sherwood Number, $D_{N_2-H_2}$ is the diffusivity in the $N_2$–$H_2$ mixture, and $d_c$ (characteristic length) is the inner diameter of the reactor: closed-ended $Al_2O_3$ tube (0.0127 m). The unit of $k^g$ is converted from SI units to match the units of $k^c$ and $k^a$:

$$k^g/RT(\text{in mol cm}^{-2}\,\text{s}^{-1}\,\text{atm}^{-1}) = k^g(\text{in m s}^{-1})\frac{10^2}{R_sT} \quad [12]$$

where $R_s$ is the gas constant (equal to 82.1 cm$^3$ atm K$^{-1}$ mol$^{-1}$) and $T$ is temperature (in K).

$D_{N_2-H_2}$ was estimated by approximating the gas as a binary mixture of nitrogen and hydrogen,[9] using the collision-integral expression from Poling *et al.*[10] The Sherwood number is calculated with Eq. [13][8]:

$$\text{Sh} = m\left(\frac{d}{r_c}\right)\text{Re}^{0.87}\text{Sc}^{0.66}, \quad (m = 0.56 \pm 0.06) \quad [13]$$

where $r_c$ is the inner radius of the closed-end $Al_2O_3$ tube (0.00635 m in current experiments), $d$ is the inner diameter of the injection tube (0.00478 m in current experiments), Re is the Reynolds number (calculated based on the gas speed through the injection tube, with the inner diameter of that tube as characteristic length), Sc is Schmidt number, calculated based on the viscosity, density, and diffusivity of the $N_2$–$H_2$ mixture. Eq. [13] holds if the ratio of $h$ to $d$ is smaller than a critical value, where $h$ = 0.005 m is the distance between the tip of the inlet tube and the metal surface. In these experiments, the $h/d$ ratio was just larger than the critical value, requiring adjustment of the calculated Sherwood number as follows[8]:

$$\text{Sh}_{\text{corr}} = \text{Sh}\sqrt{\frac{\left(\frac{h}{d}\right)_{\text{crit}}}{\left(\frac{h}{d_c}\right)}} \quad [14]$$

where $\left(\frac{h}{d_c}\right)_{\text{crit}}$ is calculated according to Eq. [16] in Saito *et al.*[8].

The viscosity of the $N_2$–$H_2$ mixture $(\mu_{N_2-H_2})$ was calculated based on the molar fractions, densities, and viscosities of pure $N_2$ and $H_2$,[11] using Wilke's equation for ideal binary gas mixture.[12] The calculated diffusion coefficient and viscosity, Reynolds number, Schmidt number, Sherwood number, corrected Sherwood number, and gas phase mass transfer coefficient for the current experiments are listed in Table II.

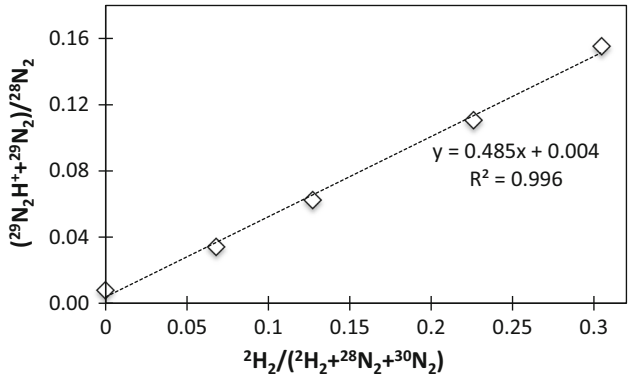


Fig. 2—Measured intensity of $m/z$ = 29 peak relative to that of the intensity of $m/z$ = 28 peak as a function of $H_2$ molar fraction in the $H_2$-$N_2$ mixture.

## III. RESULTS

### A. *Samples*

Figures 3(a) through (c) show a typical alloy sample (side, top and bottom views) after an isotope exchange experiment. The sample shows metallic luster, without any impurities visible to the naked eye.

The impurity levels of the samples from Exp. IV (0 wt pct Mn and 6 wt pct Mn) and the electrolytic iron and manganese used in these experiments are shown in Table III.

**Table II. Estimated Diffusion Coefficient and Viscosity of $N_2$–$H_2$ Mixtures, with the Reynolds Number, Schmidt Number, Sherwood Number, Corrected Sherwood Number Based on Experimental Geometry, and Gas Phase Mass Transfer Coefficient of Current Experiments**

| Flow Rate (mL/min) | Temperature (K) | $D_{N_2-H_2}$ ($m^2\ s^{-1}$) | $\mu_{N_2-H_2}$ ($kg\ m^{-1}\ s^{-1}$) | Re | Sc | Sh | $Sh_{corr}$ | $k^g$ ($m\ s^{-1}$) | $k^g/RT$ ($mol\ cm^{-2}\ s^{-1}\ atm^{-1}$) |
|---|---|---|---|---|---|---|---|---|---|
| 60 | 1873 | $1.65 \times 10^{-4}$ | $6.05 \times 10^{-5}$ | 4.32 | 0.24 | 0.58 | 0.49 | $6.39 \times 10^{-2}$ | $4.16 \times 10^{-5}$ |
| 60 | 1923 | $1.72 \times 10^{-4}$ | $6.16 \times 10^{-5}$ | 4.25 | 0.24 | 0.57 | 0.48 | $6.54 \times 10^{-2}$ | $4.14 \times 10^{-5}$ |
| 60 | 1973 | $1.80 \times 10^{-4}$ | $6.26 \times 10^{-5}$ | 4.18 | 0.24 | 0.57 | 0.47 | $6.69 \times 10^{-2}$ | $4.13 \times 10^{-5}$ |
| 75 | 1923 | $1.72 \times 10^{-3}$ | $6.17 \times 10^{-5}$ | 5.49 | 0.23 | 0.70 | 0.65 | $8.85 \times 10^{-2}$ | $5.61 \times 10^{-5}$ |
| 90 | 1923 | $1.72 \times 10^{-3}$ | $6.17 \times 10^{-5}$ | 6.74 | 0.22 | 0.83 | 0.83 | $1.13 \times 10^{-2}$ | $7.14 \times 10^{-5}$ |

**Table III. Analysis Results of O, S, Se, and N (Mass Basis) in Samples, Measured After Isotope Exchange Experiments (Experiment IV), Together with the Measured Purity of Electrolytic Iron and Electrolytic Manganese Used in the Experiments**

| Sample | S | O | Se | N |
|---|---|---|---|---|
| Exp. IV 0 Wt Pct Mn | 30 ppm | 30 ppm | | |
| Exp. IV 6 Wt Pct Mn | 30 ppm | < 20 ppm | < 50 ppm | 490 ppm |
| Electrolytic Fe | 10 ppm | 70 ppm | | |
| Electrolytic Mn | 210 ppm | < 270 ppm | | |

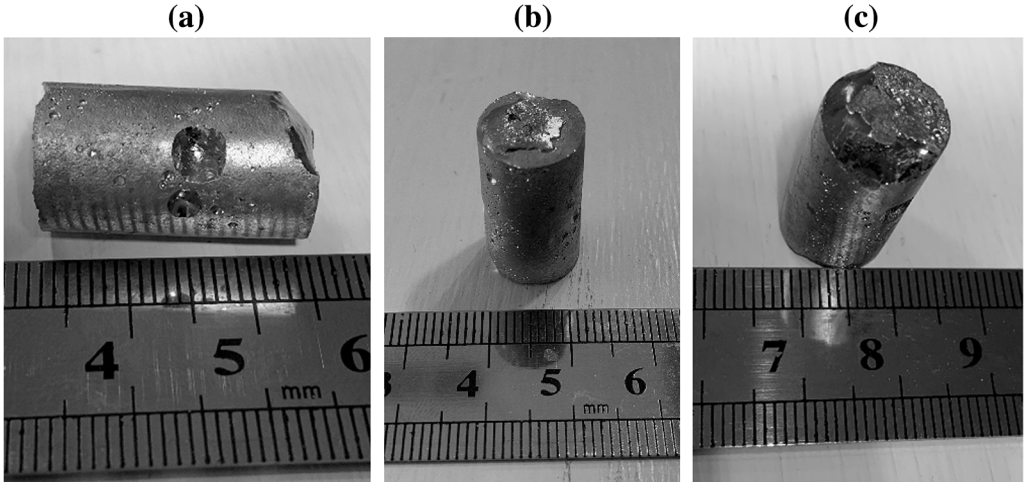


Fig. 3—Photos of (*a*) side, (*b*) top, and (*c*) bottom views view of a 10 wt pct Mn sample, after an isotope exchange experiment.

## B. *Blank Experiment*

A blank (control) experiment was conducted to test whether nitrogen isotope exchange occurred on the surface of the reactor ($Al_2O_3$ tube). Figure 4 shows the measured $^{30}N_2$/total $N_2$ ratios for Exp. I (isotope exchange in an empty reactor) and Exp. II (isotope exchange at the surface of pure liquid iron at different flow rates). Compared with Exp. I, Exp. II showed a clear step change of the $^{30}N_2$/total $N_2$ ratio when switching between the bypass circuit and the furnace circuit, indicating a measurable extent of isotope exchange in Exp. II. In contrast, the isotope exchange inside an empty reactor (Exp. I) was negligible. This confirms that the isotope exchange observed in Exp. II indeed occurred at the surface of pure liquid iron.

Figure 4 shows a difference of the baseline $^{30}N_2$/total $N_2$ ratio for the blank experiment and the experiment for the pure iron. Rather than achieving the same pct $^{30}N_2$ in each experiment (which would have required lengthy adjustment of the $^{30}N_2$ mass flow controller), the baseline concentration was measured directly. Based on the isotope exchange theory, the $^{30}N_2$ concentration in the unreacted $N_2$ mixture (baseline) does not affect the apparent rate constant $k^a$.

## C. *Effect of the Total Flow Rate*

The interfacial rate constant ($k^c$) was calculated by correcting the measured (apparent) rate constant ($k^a$) for the gas mass transfer resistance (quantified with the gas mass transfer coefficient, $k^g$). Figure 5 shows that the

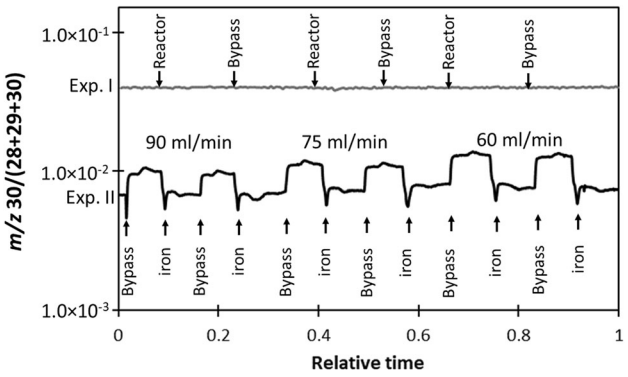


Fig. 4—Measured fractions of $m/z$ 30 ($^{30}N_2^+$) out of $m/z$ 28 + 29 + 30 ($^{28}N_2^+$ + $^{28}N_2H^+$ + $^{29}N_2^+$ + $^{30}N_2^+$) during Experiments I and II. The first two switches (from the bypass circuit to the furnace circuit) were measured at a total flow rate of 90 mL/min, the third and fourth at 75 mL/min, and the fifth and sixth at 60 mL/min.

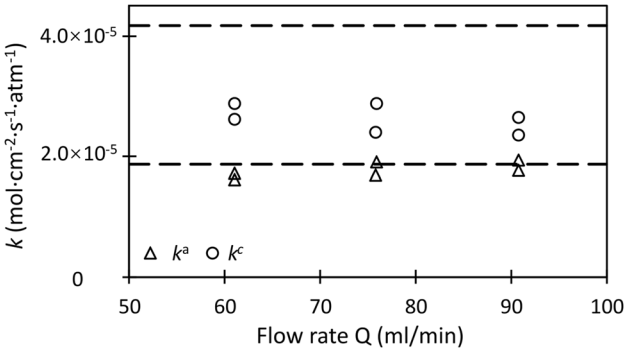


Fig. 5—Calculated apparent rate constant $k^a$ and interfacial reaction rate constant $k^c$ for pure liquid iron measured at different total flow rates (60, 75 and 90 mL/min) at 1650 °C. $k^a$ was measured twice at each flow rate. The dotted lines represent the range of previously reported $k^c$ values.[3, 4, 6, 13–16]

calculated $k^c$ (mol cm$^{-2}$ s$^{-1}$ atm$^{-1}$) for pure liquid iron at different flow rates (Exp. II) agree with each other, giving an average value of $2.6 \times 10^{-5}$ mol cm$^{-2}$ s$^{-1}$ atm$^{-1}$ at 1650 °C. The apparent rate constant $k^a$ is slightly higher at 90 mL/min, while the interfacial rate constant $k^c$ is slightly lower at 90 mL/min, which indicates that the gas mass transfer resistance might be over-estimated. The two broken lines in Figure 5 represent the literature range of reported $k^c$ values, for a slightly lower temperature (1600 °C).[3, 4, 6, 13–16] The $k^c$ values measured in this work lie within the reported range.

When applying a higher flow rate, the difference of $^{30}N_2$ between the bypass circuit and the furnace circuit was smaller, with the result that fluctuations of the incoming $^{30}N_2$ concentration caused larger measurement errors. On the other hand, when applying a low flow rate, the measured $k^a$ would be limited predominantly by gas phase mass transfer instead of the interfacial reaction. As shown in Figure 5, the $k^c$ measured at the lowest flow rate of 60 mL/min was close to the values obtained at the higher flow rates (75 and 90 mL/min). In order to maximize the difference of $^{30}N_2$ concentration between the bypass circuit and the furnace circuit, 60 mL/min flow rate was selected for subsequent experiments for liquid steel with different levels of manganese and with a Third-Generation AHSS composition.

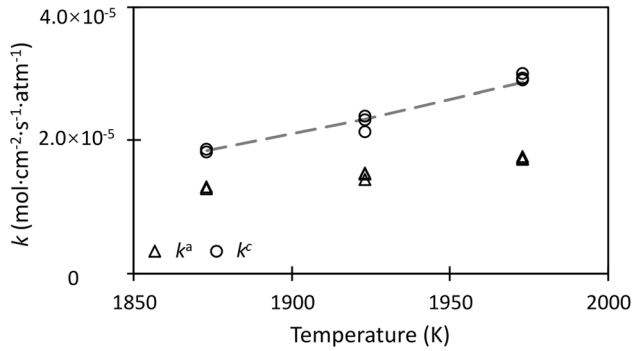


Fig. 6—Apparent rate constant $k^a$ and interfacial rate constant $k^c$ measured at different temperatures (Exp. III) for pure iron. The broken line shows the fitted temperature dependence of $k^c$, giving an activation energy of 144.2 kJ/mol.

## D. *Effect of Temperature*

The rate constant for chemisorption of a gas on a uniform surface, for either collision theory or activated complex theory for a mobile complex is given by[6]:

$$k^c = (2\pi MRT)^{-\frac{1}{2}} \exp\left(-\frac{E}{RT}\right) \quad [15]$$

where $M$ is the molecular weight of the gas (g/mol), $E$ is the activation energy (J/mol), $R$ is the gas constant (8.314 J mol$^{-1}$ K$^{-1}$), and $T$ is the temperature (K). Figure 6 shows $k^c$ measured at different temperatures (on the pure liquid iron). The broken line shows the fitted temperature dependence according to Eq. [15], giving an activation energy of 144.2 kJ/mol. As a comparison, Byrne and Belton calculated the activation energy as 145.4 kJ/mol.[6] Notice that $k^c$ measured here ($2.3 \times 10^{-5}$ mol cm$^{-2}$ s$^{-1}$ atm$^{-1}$) is smaller than that in measured in the experiment for flow rate comparison ($2.6 \times 10^{-5}$ mol cm$^{-2}$ s$^{-1}$ atm$^{-1}$), possibly indicating that the impurity levels (S and O) in these two experiments are different, or the temperature measurements are inaccurate in Exp. I. The estimated errors in the rate constant (see the section "Error analysis" for the estimation procedure) are too small to be visible as error bars in Figures 6, 7, and 8.

## E. *Effect of Manganese*

Manganese is a major alloy element in many steel grades. Understanding how manganese influences the kinetics of nitrogen reaction can benefit nitrogen control in the steelmaking process. Figure 7 shows $k^c$ measured at different temperatures for different Mn concentrations (0, 6 and 10 wt pct). Similar to $k^c$ measured on the pure liquid iron, a positive dependency of $k^c$ on

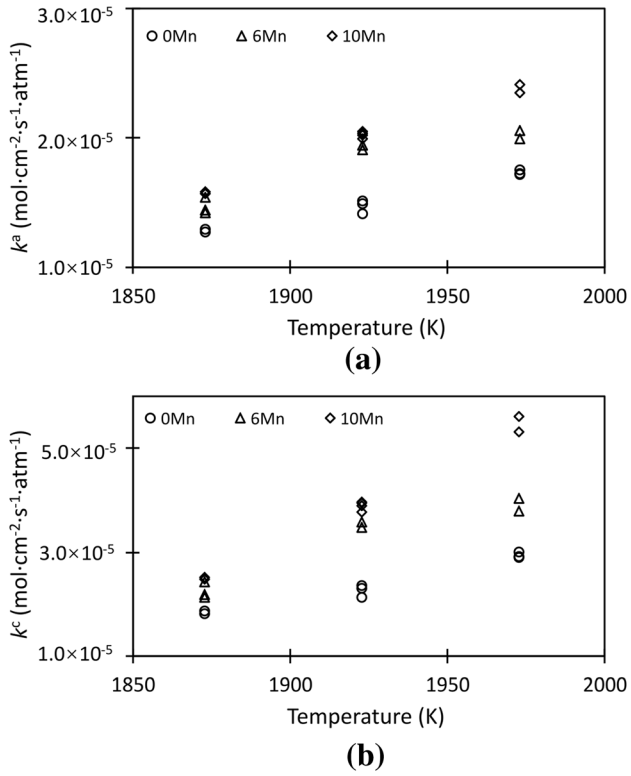


Fig. 7—(*a*) Measured apparent rate constant $k^a$ and (*b*) corrected interfacial reaction rate constant $k^c$ (mol cm$^{-2}$ s$^{-1}$ atm$^{-1}$) on Fe-Mn containing 0, 6, and 10 wt pct Mn (Exp. IV).

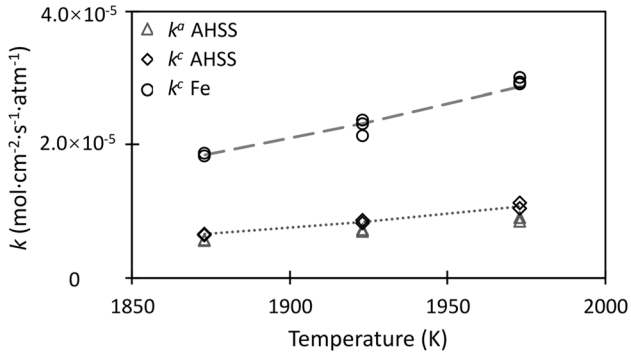


Fig. 8—Apparent rate constant and interfacial reaction rate constant measured at different temperatures for a Third-Generation AHSS steel composition (0.5 Al 1.5 Si 6 Mn 92 Fe; based on Exp. V), showing $k^c$ for pure iron for comparison. The broken line shows the fitted temperature dependence of $k^c$, giving an activation energy of 144.2 kJ/mol for pure iron and 160.5 kJ/mol for the AHSS composition.

temperature is observed for different [Mn] contents. The measured $k^c$ also increases with increased [Mn]. Notice that at 10 wt pct, the measured apparent rate constant $k^a$ at 1973 K is approximately half of the gas phase mass transfer resistance $k^g$, resulting in a significant correction (for gas phase mass transfer resistance) and a much higher $k^c$.

### F. *Rate Constant for a 3rd Gen AHSS steel*

The measured interfacial rate constant ($k^c$) for liquid steel with a 3rd Gen AHSS composition (listed in Table I, Exp. V) was significantly lower than for pure iron (Figure 8). The calculated activation energy is 160.5 kJ/mol, compared to 144.2 kJ/mol for pure iron. Though Mn has a positive effect on the interfacial reaction rate $k^c$ (Figure 7), both Al and Si have the opposite effects.[14]

In previous work, the effect of an alloying element $x$ on $k^c$ was linked to the interaction coefficients between $x$ and nitrogen, where $x$ represents elements such as Mn, Al, and Si. For simplification, only the first-order interaction coefficient is considered $\left(e_{\mathrm{N}}^{x}\right)$. A positive first-order interaction coefficient indicates that the alloying element interacts less strongly with nitrogen than Fe; a negative value indicates that alloying element $x$ interacts more strongly with nitrogen, lowering its activity coefficient. It was proposed that a negative interaction coefficient correlates with a higher liquid metal–nitrogen interfacial reaction rate[2–4] (while also increasing nitrogen solubility). At least as far as the measured manganese effect is concerned, the current work agrees with this trend $\left(e_{\mathrm{N}}^{\mathrm{Mn}} = -0.023\right)$.[17]

### G. *Error Analysis*

As shown earlier, the apparent rate constant $k^a$ is calculated as follows:

$$k^a = -\frac{\bar{V}}{AR_sT}\ln\frac{{}^{30}F_f - {}^{15}f^{15}f}{{}^{30}F_i - {}^{15}f^{15}f} \qquad [2]$$

The error in the measured $k^a$ ($\sigma_{k^a}$) is defined as

$$\pm\sigma_{k^a} = k^{a'} - k^a \qquad [16]$$

where $k^{a'}$ is the measured apparent interfacial reaction rate constant and $k^a$ is the actual apparent interfacial reaction rate constant.

The four values that are measured during the experiment are $\bar{V}$ (volumetric gas flow rate), $T$ (the temperature), ${}^{30}F_f$ (fraction of ${}^{30}\mathrm{N}_2$ in the gas mixture after reaction), and ${}^{30}F_i$ (fraction of ${}^{30}\mathrm{N}_2$ in the gas mixture before reaction). From Eq. [2], if there is any deviation of measured $\bar{V}$ and $T$ from the real value, the deviation ($\sigma_{k^a}$) of the measured $k^a$ would be proportional to that of $\bar{V}$ and $1/T$. However, since the same experimental setup and flow rate were used—$\bar{V}$ (50 mL/min for natural abundance nitrogen + 10 mL/min hydrogen) and $T$ (1600, 1650 and 1700 °C)—the trend of $k^a$ with changing alloy concentration would not be affected by errors in flow rate or temperature measurement (that is, the same systematic errors would affect experiments performed with different gas compositions). However, errors in the measured values of ${}^{30}F_i$ and ${}^{30}F_f$ can affect the results. If the incoming gas mixture contains no ${}^{29}\mathrm{N}_2$, and writing ${}^{30}F_i$ as $x$ and the difference between ${}^{30}F_i$ and ${}^{30}F_f$ as $\Delta x$,

$$^{30}F_i = x \quad [17]$$

$$^{30}F_i - {}^{30}F_f = \Delta x \quad [18]$$

then Eq. [2] can be rewritten as

$$k^a = \frac{-\bar{V}}{ART}\ln\left(1 + \frac{\Delta x}{x^2 - x}\right) \quad [19]$$

From Eq. [19], a smaller total flow rate, a larger surface area, and a larger $^{30}F_i$ ($x$, only for $x$ smaller than 0.5) will lead to a larger, more readily measurable $\Delta x$. As reported earlier, this flow rate effect was found experimentally.

For errors from measuring $^{30}N_2$, let $\delta$ represent the relative error:

$$\delta = \frac{\sigma}{x} \quad [20]$$

Here, $\sigma$ represents the standard deviation of measured $^{30}F$, which is mainly due to unstable flow (from the mass flow controllers), possible incomplete mixing of $^{30}N_2$ and $^{28}N_2$, and possible pressure fluctuations inside the RGA chamber. Better flow control would give smaller $\sigma$. To simplify the calculation, it is assumed that the error in the measured baseline $^{30}N_2$ is zero ($^{30}\sigma_i = 0$, for example when using a pre-mixed gas). Then the deviation ($\sigma_{k^a}$) of measured $k^a$ caused by $\delta$ can be expressed as

$$\pm\sigma_{k^a} = k^{a'} - k^a = \frac{-\bar{V}}{ART}\ln\left(1 \pm \frac{\delta(x - \Delta x)}{x^2 - (x - \Delta x)}\right) \quad [21]$$

As $x$ and $\delta$ are both small, the above equation can be rewritten as

$$\pm\sigma_{k^a} = k^{a'} - k^a = \frac{-\bar{V}}{ART}\ln(1 \mp \delta) \quad [22]$$

The above equation can be further simplified as

$$\pm\sigma_{k^a} = k^{a'} - k^a = \pm\frac{\bar{V}\delta}{ART} \quad [23]$$

From Eq. [23], a higher flow rate and a lower surface area will both increase $\sigma_{k^a}$. This is the primary reason why a relatively low total flow rate (60 mL/min) was selected for most of the experiments.

The value of $\sigma_{k^a}$ calculated this way was less than 4 pct of the rate constant. $\sigma_{k^a}$ can be further minimized by achieving a constant $^{30}F_i$ by using a pre-mixed gas. Also, if it is applicable, a reactor with a larger diameter is suggested for these experiments so that the surface area could be larger. However, the repeatability of the experiment was previously reported to be low: when a repeated experiment is conducted with the same experimental setting, the measured $k^a$ can change up to 20 pct.[6] This may be due to fluctuations of impurity levels in the steel sample.

## IV. CONCLUSIONS

The nitrogen-liquid steel interfacial reaction rate $k^c$ was measured using isotope exchange experiments. Compared with the Byrne and Belton's classic experiment, certain modifications were made in the current experiment setup, including introducing a bypass gas line, using a graphite susceptor for induction heating, and using a closed-end tube as a reactor. The standard deviation from one measurement to another in a single experiment was calculated to be relatively small (< 4 pct), but the fluctuations in levels of impurities (S, O, and Se) in the raw metal likely influenced the repeatability of the experiments.

Overall, the conclusion is that the measured $k^c$ for pure iron falls within the range of literature data, whereas Mn accelerates the interfacial nitrogen reaction. In contrast, steel with a Third-Generation AHSS composition had a lower $k^c$ compared to pure iron, apparently due to the retarding effect of Al and Si.

## ACKNOWLEDGMENTS

Support of this work by the industrial members of the Center for Iron and Steelmaking Research is gratefully acknowledged.

## REFERENCES

1. B. Hu, H. Luo, F. Yang, and H. Dong: *J. Mater. Sci. Technol*, 2017, vol. 33, pp. 1457–64.
2. H. Ono, K. Morita, and N. Sano: *Metall. Mater. Trans. B*, 1995, vol. 26B (10), pp. 991–95.
3. H. Ono, T. Koyama, and T. Usui: *ISIJ Int.*, 2003, vol. 43 (3), pp. 298–303.
4. S.M. Han, J.H. Park, S.M. Jung, J.H. Park, and D.J. Min: *ISIJ Int.*, 2009, vol. 49 (4), pp. 487–94.
5. P.C. Glaws and R.J. Fruehan: *Metall. Mater. Trans. B*, 1986, vol. 17B, pp. 317–322.
6. M. Byrne and G.R. Belton: *Metall. Trans. B*, 1983, vol. 14B, pp. 441–49.
7. E.P.L. Hunter and S.G. Lias: *J. Phys. Chem. Ref. Data*, 1998, vol. 27 (3), pp. 413–56.
8. H. Saito, A. Yoshizawa, and T. Soma: *Tetsu-to-Hagane*, 1984, vol. 70 (1), pp. 58–64.
9. B.E. Poling, J.M. Prausnitz, and J.P. O'Connell: *Properties of Gases and Liquids*, 5th ed., McGraw-Hill Education, New York, 2001.
10. P.D. Neufeld, A.R. Janzen, and R.A. Aziz: *J. Chem. Phys.*, 1972, vol. 57 (3), pp. 1100–1102.
11. P.B. Bird, E.N. Lightfoot, and W.E. Stewart: *Transport Phenomena*, Wiley, New York, 2007.
12. C.R. Wilke: *J. Chem. Phys.*, 1950, vol. 18 (4), pp. 517–19.
13. A. Kobayashi, F. Tsukihashi, and N. Sano: *ISIJ Int.*, 1993, vol. 33 (11), pp. 1131–35.
14. K. Morita, T. Hirosumi, and N. Sano: *Metall. Trans. B*, 2000, vol. 31 (5), pp. 899–904.
15. T. Nagasaka, R. J. Fruehan and A. W. Cramb: *ISSTech 2003 Proc.* Iron and Steel Society, 2003, pp. 979-992.
16. J. Lee and K. Morita: *ISIJ Int.*, 2003, vol. 43 (1), pp. 14–19.
17. D. Senk, K. Christmann, S. Geimer, and D. Rzehak: *Steel Res.*, 2016, vol. 87 (1), pp. 107–111.